Cell Biochem Biophys (2008) 52:113–124
DOI 10.1007/s12013-008-9028-1

ORIGINAL PAPER

Modelling the Role of Intrinsic Electric Fields in Microtubules as an Additional Control Mechanism of Bi-directional Intracellular Transport

M. V. Sataric · L. Budinski-Petkovic · I. Loncarevic · J. A. Tuszynski

Published online: 2 October 2008

Abstract Active transport is essential for cellular function, while impaired transport has been linked to diseases such as neuronal degeneration. Much long distance transport in cells uses opposite polarity molecular motors of the kinesin and dynein families to move cargos along microtubules. It is clear that many types of cargo are moved by both sets of motors, and frequently in a reverse direction. The general question of how the direction of transport is regulated is still open. The mechanism of the cell's differential control of diverse cargos within the same cytoplasmic background is still unclear as is the answer to the question how endosomes and mitochondria move to different locations within the same cell. To answer these questions we postulate the existence of a local signaling mechanism used by the cell to specifically control different cargos. In particular, we propose an additional physical mechanism that works through the use of constant and alternating intrinsic (endogenous) electric fields as a means of controlling the speed and direction of microtubule-based transport. A specific model is proposed and analyzed in this paper. The model involves the rotational degrees of freedom of the C-termini of tubulin, their interactions and the coupling between elastic and dielectric degrees of freedom. Viscosity of the solution is also included and the resultant equation of motion is found as a nonlinear elliptic equation with dissipation. A particular analytical solution of this equation is obtained in the form of a kink whose properties are analyzed. It is concluded that this solution can be modulated by the presence of electric fields and hence may correspond to the observed behavior of motor protein transport along microtubules.

Keywords Microtubule · Tubulin · GTP · Kinesin · Dynein · Kink · Ferroelectric

M. V. Sataric · L. Budinski-Petkovic · I. Loncarevic
Faculty of Engineering, University of Novi Sad, Trg D. Obradovica 6, 21000 Novi Sad, Serbia

J. A. Tuszynski (✉)
Experimental Oncology, Cross Cancer Institute, 11560 University Avenue, Edmonton, Alberta T6G 1Z2, Canada
e-mail: jtus@phys.ualberta.ca

Ferroelectric Properties of Microtubules

The methods of biochemistry have been instrumental in advancing our knowledge of cell biology over the past several decades. However, they mostly focus on binary interactions between proteins and other biomolecules. Biochemistry also considers various complicated signal transduction pathways to evoke long-range effects or responses, but some difficulties still persist in explaining various long-range effects that undoubtedly take place in cells. We believe that electrostatic and electrodynamic effects may play a much greater role in cell processes than hitherto assumed. It is known that associated proteins such as dynactin, klar, and rabs play a role in switching kinesin and dynein molecules on or off. However, this does not exclude the possibility that these interactions could be initiated, affected, or time- and space-ordered by moving ionic waves or dipole moment changes brought about by propagating kinks with a finely tuned amplitude and speed. A propagating kink wave moving in one direction could cause a kinesin molecule to switch on or off depending on the particular situation. In this connection, dipole moments and ferroelectric properties of biomolecules may be of crucial importance.

Large polar molecules, ferroelectric (FE) polymers, and ferroelectric/ferroelectric liquid crystals, represent

electrically active materials that are crucially important in many functions of living cells and have a great potential for biotechnology applications. It has been suggested that ferroelectricity and pyroelectricity is an essential and universal property of biomaterials [1]. There is a substantial body of evidence suggesting FE mechanisms for a number of biological processes such as conducting membrane functions [2], memory [3], and post-synaptic membrane function [4]. Two decades ago Kubisz et al. [5] investigated FE and ferroelectric properties of collagen [6]. It is very likely that the documented ferroelectricity of bone material and tendon is largely due to the presence of collagen in these structures [7]. Leuchtag and Bystrov [8] edited a collection of papers on Ferroelectric and Related Models in Biological Systems which focused on two types of biological structures suspected of having FE properties (a) microtubules and (b) voltage-dependent ion channels. Both types of structures are proteins involved with signaling and information processing at the cell level.

The idea that microtubules (MTs) are ferroelectric was proposed over 20 years ago [9]. This was then quantitatively modeled by Satarić et al. [10] on the basis of ferroelectric properties of MTs and improved by the newly acquired knowledge of the detailed secondary and tertiary structures of tubulin (see Fig. 1) [11, 12].

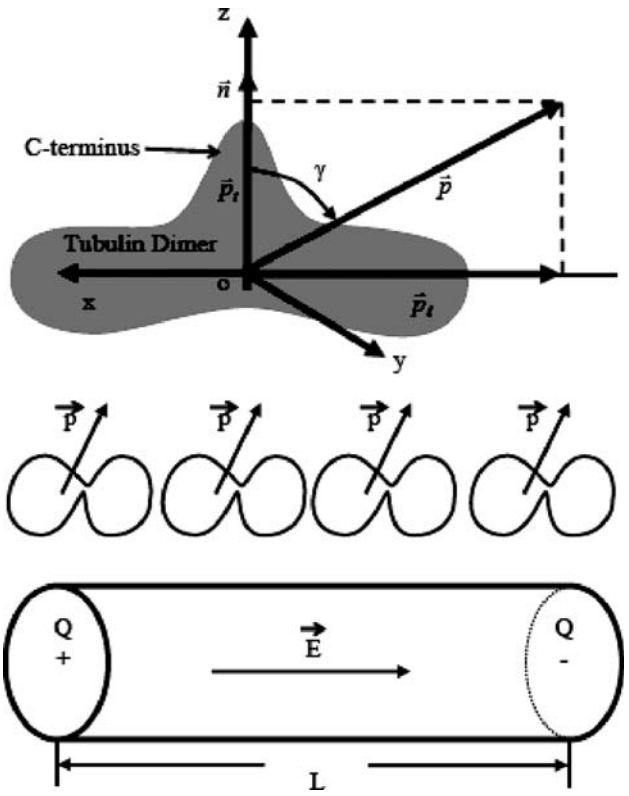

Fig. 1 An individual dimer with its dipole decomposed, a protofilament with the dipoles of individual dimers, and a MT with the giant dipole due to these individual contributions

The cytoskeleton consists of three major types of thin rod-like filaments that span the cytoplasm: actin-based filaments (i.e., microfilaments), tubulin-based filaments (i.e., microtubules), and intermediate filaments (e.g., neurofilaments, keratin). There are at least three well-studied mechanical functions of the cytoskeleton in vivo: providing the mechanical strength of the cell, segregating the chromosomes, and participating in the transport of macromolecules via motor proteins [13]. Microtubules are formed as a ferroelectric polymer whose building block is a protein called tubulin. A microtubule is a hollow cylindrical structure whose wall is made up of parallel chains, or protofilaments, of tubulin hetero-dimer molecules longitudinally shifted from each other so as to result in a helical structure. Each dimer, 8 nm in length, is composed of two units, an α- and a β-tubulin monomer. Each MT is generally made up of 13 protofilaments which results in an outer diameter of $\sim$25 nm, and the length that varies from microns to centimeters [10]. In addition to providing structural strength and flexibility to the cells, MTs guide and transport cellular material toward or away from the center of the cell (see Sec. 3), play a key role in cell division, and are also believed to be involved in intracellular signaling [14]. A number of authors have suggested that these functions can be understood based on the hypothesis that MTs exhibit FE-like properties [10, 14, 15].

Table 1 summarizes the results of calculations [16] of tubulin's net charge and the dipole moment using the data from the entry 1TUB in the PDB (protein Data Bank), i.e. excluding the C-termini that are known to account for approximately 40% of the total charge of the protein. The x-direction in Table 1 coincides with the MT protofilament axis. The y-axis is oriented radially toward the MT center and the z-axis is tangential to the MT surface.

The MT structure can be viewed as a FE system with the dipole moments of tubulin oriented roughly perpendicularly to the MT surface [16]. Figure 2 illustrates the MT with the axes labeled. While much of the dipole moments cancel due to the cylinder's rotational symmetry with regard to its axis, a net axial component remains as the ends of a MT exhibit a different net charge [17]. Thus, the

Table 1 Key electrostatic properties of tubulin based on the Nogales structure excluding the C-termini

Tubulin properties	Dimer	α-Monomer
Charge (electron units)	−10	−5
Dipole (Debye)		
Overall magnitude	1714	556
x-component	337	115
y-component	−1669	554
z-component	198	−6

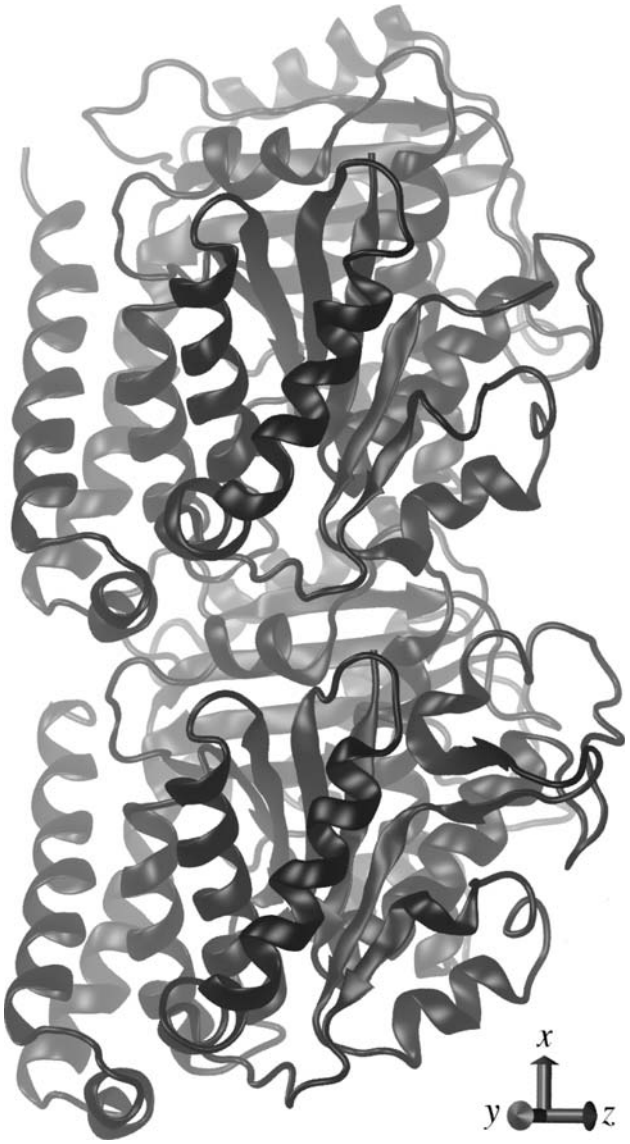

Fig. 2 The coordinate axes in the 1TUB and 1JFF data sets relative to tubulin orientation in a microtubule. The dimer is oriented so that the microtubule axis runs up–down the page and a radial vector outward from the microtubule center is toward the left edge of the image. Note the rotation about the yz-plane relative to the zinc-induced sheet axes. Image prepared with VMD [69]

MT cylinder supports an intrinsic electric field, E, giving it an axial polarity, as has been known to biologists for a long time. Interestingly, Maniotis et al. [18] and others demonstrated that MTs can transduce mechanical forces over micron-long distances inside the cell, even into the nucleus, suggesting an efficient signaling phenomenon that can be related to MT ferroelectricity.

In proteins, virtually every peptide group in an a-helix possesses a dipole moment on the order of $p_0 = 1.2 \times 10^{-29}$cm (=3.5 Debye). Being almost parallel to the helical axis these dipole moments give rise to an overall large dipole moment of this particular helix which plays an important biological role [9]. Since the tubulin dimer contains several α-helices which are not oriented randomly, it is not surprising that each tubulin dimer possesses a large net dipole moment. Tuszyński et al. [16, 19] have recently recalculated the values of the dipole moments and net charges using the sequences of the various homologous isotypes of tubulin. In order to experimentally determine the dipole moment of tubulin, Mershin et al. [20] and Schuessler et al. [21] performed a surface plasmon resonance study on tubulin dimers in solution. Analysis of their data yielded for tubulin a refractive index $n = 2.9$ and hence a dielectric constant $\varepsilon(=n^2) = 8.4$ and $|p| \approx 1,000$ Debye which agrees with the order of magnitude of the calculated dipole moment.

Finally, there have been some preliminary experiments aimed at measuring the electric field around MTs [22, 23] indicating that MTs could be FE. Stracke et al. [24] applied moderate electric fields to suspended MTs and to MTs gliding across a kinesin-coated glass surface. In suspension, MTs without MAPs moved from the negative to the positive electrode at a pH of 6.8, indicating a negative net charge which has been significantly screened due to the counter ions surrounding them. Experimental evidence of a significant electric charge in tubulin has been provided in [25]. Recently, Dombeck et al. [26] used uniform polarity MT assemblies imaged in native brain tissue by second-harmonic generation microscopy which only worked for uniform polarity bundles but not for anti-parallel arrangements indicating a nonlinear polarization effect. Other than the above observations, there exists little experimental evidence concerning tubulin and MT electrical properties, especially at in vivo conditions. However, the importance of electrostatics in the behavior of microtubules, including cell division, has been discussed in detail in [27].

The idea that MTs are ferroelectric was more recently argued for by Nanopoulos et al. [28]. Due to the strong curvature of an MT cylinder, the inner parts of the dimer structure are compressed in order to fit into an MT while the outer ones are stretched out which causes additional redistribution of excess negative charge. This effect is analogous to that observed for cylindrical hair cells [29]. This has also been corroborated by a map of the electric charge distribution for the tubulin dimer obtained using molecular dynamics simulations for the tubulin structure listed in PDB [30].

The presence of oriented assemblies of dipoles in the wall of an MT can be shown to be responsible for the observed ferroelectricity of MTs [10, 14]. It has been demonstrated that it is possible to orient arrays of MTs by the application of an electric field and it has been further speculated that inter-cellular electric fields may induce MT orientation [14]. That such orientation is possible can be concluded by noting that MTs are sensitive to fields $\sim$100 mV/μm, or $\sim 10^3$ V/

cm, whereas fields measured across cellular membranes are 10^5 V/cm [10, 14]. The mentioned orientation of MTs refers to experiments in vitro. The strength of electric fields responsible for the kink's motion in our model should be much smaller than 10^3 V/cm.

A theoretical model demonstrated how coherent lattice excitations propagate coupled electrostatic and elastic energy packets via solitary waves, which originate from the hydrolysis of a guanosine triphosphate (GTP) molecule bound to the β-tubulin monomer [15]. External electric fields consistent with the axonal action potential were shown capable of reordering these local dipoles. Energy loss-free transport along MTs has been shown possible [10, 15, 31] as a result of "kink-like excitations", or solitons, as an energy-transfer mechanism in MTs. This feature arises from nonlinear coupling between the dielectric and elastic degrees of freedom of the tubulin dimers and from the inclusion of a viscous force representing the damping effect of the surrounding water molecules. Depending on the model and the parameters assumed, the speed of such waves has been estimated to be $10^{2\pm1}$ m/s [15].

Kinesin Processivity on Microtubules

The two principal motor proteins that attach to MTs are kinesin and dynein. While kinesin moves toward the plus end of a MT, dynein is negative-end directed. Each of these proteins consists of two globular head regions and an extended coiled-coil tail section linking them.

Kinesin moves from the minus toward the plus end of a MT and is a force-generating motor protein, which converts the free energy of the gamma phosphate bond of ATP into mechanical work used to power the transport of intracellular organelles along MTs. The current model force generation by motor proteins hinges on the fact that the motor contains an elastic element, a spring, that becomes strained as a result of one of the transitions between chemical states. The relief of this internal strain is the driving force for the forward movement [32]. The so-called head-over-head mechanism has been accepted as a consensus mode of operation although recently doubts have been expressed whether this is the correct picture [33–35]. Studies of motor proteins have shown that the essential components for force generation are located within each of the two globular heads.

Models of motor protein movement can essentially be divided into those with diffusion and those with a power stroke [36]. The efficient propagation of these proteins, often involving pairs such as kinesin and dynein moving simultaneously in opposite directions and seemingly avoiding collisions led to the proposal that they may be directed or controlled by electrostatic interactions with the MT [37] and it is interesting to note that the binding of kinesin to MTs has since been shown to be primarily electrostatic [38].

The diffusion models require an oscillating potential that is presumably driven by a conformation change of the motor-MT bond. Activation of the complex by ATP leads to a potential that is relatively flat. Diffusion occurs in this state and once the potential reverts to its asymmetric form, the geometry of the potential is such that forward propagation of the motor protein is favored. A review of such schemes may be found in [39]. In the power stroke models by contrast, it is the motor protein whose structure changes. The motor protein has two or more distinct states where at least one conformational change occurs and is driven by ATP hydrolysis as has been experimentally demonstrated for myosin [40]. It is interesting to note that the use of GTP to control MT dynamics and ATP to control motor protein motion along MTs, allows the cell to have control over both the cars (motor proteins) and the track (MTs) individually.

Buttiker [41] and Landauer [42] proposed a model for molecular motors which results in uni-directional motion of a molecule along a quasi-one-dimensional protein fiber. This model was essentially a generalization of the thermal ratchet model of Feynman [43]. Recent attempts at explaining the motor protein behavior use isothermal ratchets in which the motor is subjected to an external potential that is periodic and asymmetric. In addition, a fluctuating force $F(t)$ is acting on the motor. A review article on this topic [39] distinguishes three classes of such models, namely: (i) a Langevin-based approach in a constant potential [44], (ii) an approach in which the potential fluctuates in time [45], and (iii) a generalized model with several internal particle states which is described by the Langevin equation that depends on the state it is in. A more convenient and elegant approach is through the Fokker-Planck formalism [46] for the probability distribution function $P(x, t)$ that describes the motion of the motor in a statistical manner. So far, models of the above types have been fairly successful in representing the gross features of the experimental data obtained [47] although they do not address specific molecular mechanism issues.

A recent paper [48] proposed a new physical mechanism intended to describe the mode of processive motion along MT filaments for two-headed motor proteins such as kinesin. It treats the two motor domains as extended objects that are connected by a neck linker region. The head domains feel the 2D periodic potential on the surface of the MT and are also subjected to thermal noise. In the mathematical model developed in this paper, ATP hydrolysis provides the chemical energy while directed binding plays the key role in mechanical force generation coupled with the presence of a pair of torsion springs to store and release elastic energy.

Although kinesin and dynein motors are uni-directional, many cargoes move bi-directionally, reversing their course every few seconds. There are many examples of such motion. Chromosomes, mitochondria, endosomes, viruses, and various vesicles exhibit back and forth motion. Mitochondria are typically observed to move along microtubules in both directions, and appear to move to cellular locations where ATP production is needed. Indeed, many generally uni-directional cargoes may in fact have bi-directional motion with such short direction reversals that the bi-directional character of their motion may be missed. In many experiments it has been shown that both kinesin and dynein are attached to the same cargo at the same time, while none has suggested that only one set of motor proteins is bound at a time. The findings from a number of systems [49, 50] suggest that opposing motors are co-ordinated so that they tend not to interfere with each other. When dynein is active, kinesin is inactive, and vice versa. Since the mechanism of such co-ordination is unknown, we believe this paper offers an appealing and plausible insight into how such coordination may be achieved.

The Model of Tubulin Tail Kink Excitations

When Nogales et al. [51] determined a 3D structure for tubulin, the extreme carboxyterminal ends of the peptide were not crystallographically resolved since these regions seem to be highly flexible and lacking a fixed preferred conformation. Using NMR Jiminez et al. [52] have studied the helicity of isolated α and β tubulin C-terminal peptide sequences. Below we use CT as an abbreviation for the tubulin carboxy-terminus. Located on the outside of the MT, CTs interact strongly with other proteins, such as MAP2 and kinesin [53]. The processivity of kinesin appears to critically involve an interaction with CTs. CT removal profoundly affects kinesin processivity; in particular cleavage by subtilisin results in a fourfold decrease of the rate of kinesin transport [54]. However, the impact on dynein has been less extensively investigated.

Ion condensation may be expected to take place on MT CTs due to their strong negative charge, and exposure to the aqueous environment. Manning [55] developed an elegant theory that poly-electrolytes may "condense" neutralizing ions from their surroundings if a sufficiently high linear charge density is present on the polymer's surface. Although originally postulated for such poly-electrolytes as DNA, this theory applies to highly charged quasi-one-dimensional polymers such as the MT CTs. CTs have a net charge of up to 11 electrons each and interact electrostatically with: (a) the surface of the tubulin dimer (which is generally negatively charged but which also exhibits positively charged regions on its exposed surface), (b) with neighboring CTs, and (c) with adjacent proteins such as kinesin or MAP2.

Computer simulations [56] suggest that the CTs are likely to exist in two major conformational states: (a) a flexible conformation pointing away from the MT surface and subject to thermal fluctuations, or (b) a state in which CTs bind to the MT surface. Each dimer has two CTs that may either extend outward from the surface of the protofilament or bind to it. The states of the CTs may affect other sub-cellular processes, e.g. the processive motion of kinesin motor proteins transporting cargo such as mRNA as they walk on the MT. In the present paper we are interested in finding out if these states can become collectively coupled and also if they are responsive to external electric fields that may control their dynamics and hence the processivity of kinesin molecules and their cargo transport. The mass of the molecular chain of peptides comprising a CT is estimated as 2 kD. The net charge of a CT is assumed to be $-10e$. The nominal length of the CT is taken to be $L = 4.5$ nm.

β-tubulin has an exchangeable GTP site that is an active domain. The chemical potential energy of GTP hydrolysis is proposed to be converted into mechanical motion as follows. The dissociation of the inorganic phosphate group (P_γ) in the reaction ($GTP \rightarrow GDP + P_\gamma$) causes a shift of a few angstroms in the GTP binding site that contains a polypeptide protruding loop called a sensor or switch loop. This displacement could then cause a further conformational change that propagates along a tightly associated α-helix called the relay-helix (RH). This serves as a 'piston' that transmits the sensor stimulus to a site on the opposite side of the same β-tubulin latching it in a "closed" conformation. See Fig. 3 for two views of the tubulin dimer.

This state of the RH corresponds to that of a pre-stressed spring, to use a mechanical analogy. This transformation is evolutionarily consistent with the conformational strategies exhibited by motor proteins due to ATP hydrolysis [57]. We propose that as a next stage in the conformational transformation of β-tubulin, triggered by the unlatching of the RH, an α-helix (H12) is pushed, which causes the connected CT to rotate by θ in the (x, r)-plane as shown in Fig. 4. The released RH force estimated in [58] results in the CT tilting by the angle $\theta \approx 0.5$ rad. We have also calculated the work done by the piston-like RH translation to be approximately $2 \times 10^{-20}\text{J} \approx 0.13$ eV. Since the energy released in one GTP hydrolysis event is about 0.25 eV it follows that most of it would be used in the tilting of the CT [59].

Therefore, we treat a β-tubulin CT after GTP hydrolysis as a rotational pendulum with respect to the tilt angle θ, and with the corresponding CT rotational inertia

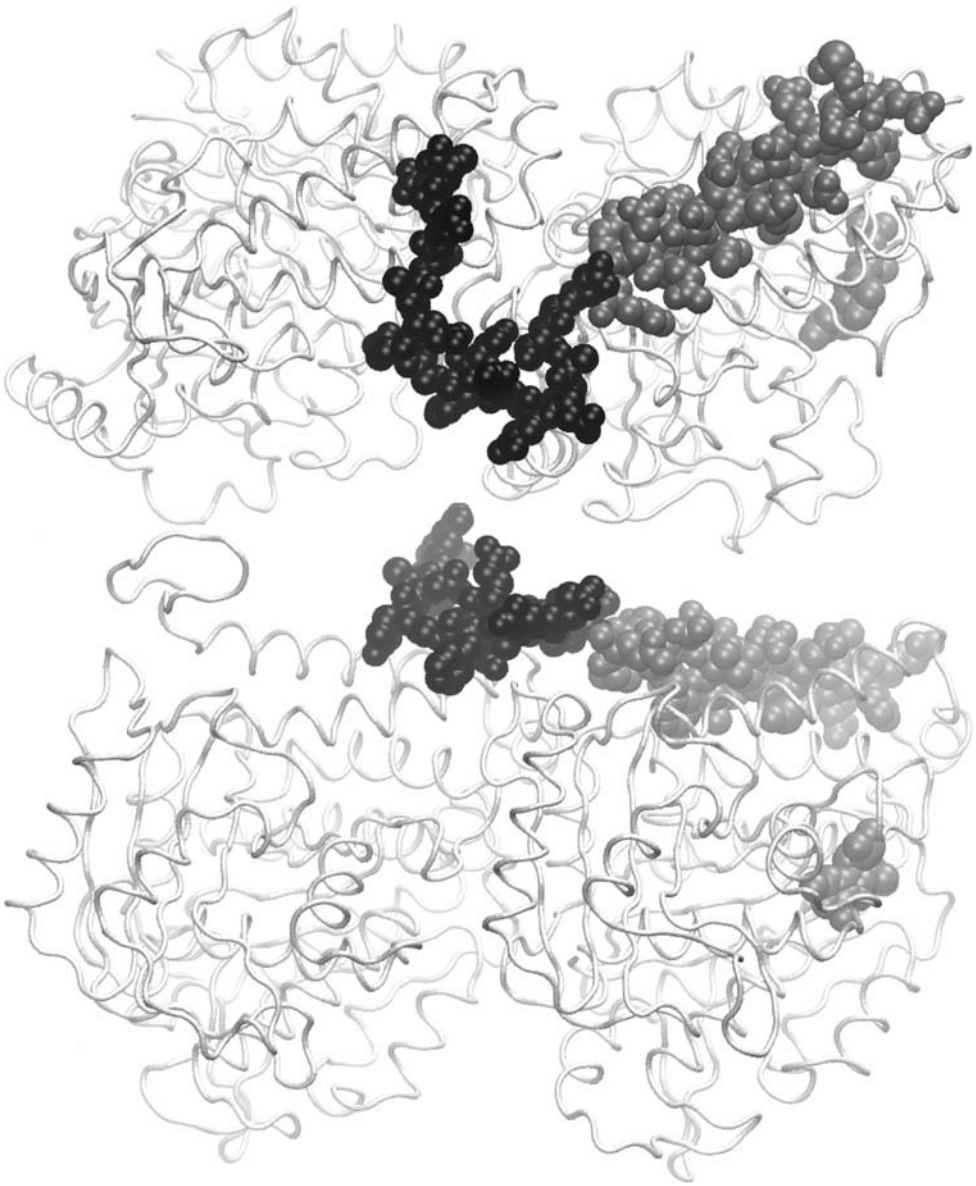

Fig. 3 Two views of a tubulin dimer with 90° rotation between them, showing the location of guanosine-phosphates, Helix 12, and the C-terminal tail. The tail is the darker (horizontally centered) collection of balls and H-12 the adjacent lighter toned group. The guanosine-phosphate is the smaller group near the right edge and below the H12 collection in both views. In both images the microtubule axis runs left–right. A radial vector from the microtubule center is toward the viewer in the upper image and up the page in the lower image. Image prepared with VMD [69]

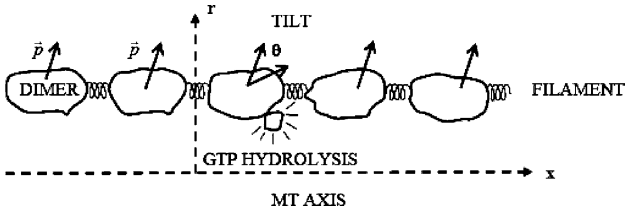

Fig. 4 GTP hydrolysis creates a piston-like movement which causes significant tilt of the tubulin dimer's CT

per unit volume J, possessing the kinetic energy density given by

$$w_{\text{kin}} = \frac{1}{2} J \left(\frac{\partial \theta}{\partial t} \right)^2 \tag{1}$$

The splay elastic energy density has the form

$$w_{\text{sp}} = \frac{1}{2} \kappa \left(\frac{\partial \theta}{\partial x} \right)^2 \tag{2}$$

where κ denotes the splay elastic modulus.

Crucial to the total CT energy, is the energy of CT–CT coupling within a protofilament. If we ignore the differences in the mass and shape of CTs between α and β-monomers we can expand this energy in terms of the tilt angle θ as an even function, up to the fourth order as follows:

$$w_{\text{coup}} = \frac{1}{r^2} \left(-A\theta^2 + B\theta^4 \right) \tag{3}$$

where A and B are coefficients that are expressed in terms of cylindrical components of the elasticity tensor, and r is the radial co-ordinate along with CTs. The reason for

expanding the energy to the fourth order is that the triggering tilt angle ranges up to $\theta_0 \approx 0.5$ rad leading to $\theta^4 \approx \frac{1}{16}$, which is not negligible when compared to the $\theta^2 \approx \frac{1}{4}$ term.

The last part of the total CT pendulum energy considered here is the polarization energy density:

$$w_{\text{pol}} = \frac{1}{2}\left(\frac{p_{\text{l}}^2}{\chi_{\text{l}}} + \frac{p_{\text{t}}^2}{\chi_{\text{t}}}\right) - p_{\text{l}}E - \mu_{\text{p}}p_{\text{t}}\theta \tag{4}$$

where p_{l} and p_{t} are longitudinal and transverse projections of the tubulin polarization, χ_{l} and χ_{t} are the anisotropic dielectric susceptibilities of a MT, while μ_{p} is a phenomenological model parameter, and E the intrinsic electric field within a MT (see Fig. 1).

We also account for viscosity of the medium surrounding the MT (cytosol). This was modeled by including a friction term in the equation of motion, by the corresponding torque

$$\tau_{\text{vis}} = -\Gamma\frac{\partial\theta}{\partial t} \tag{5}$$

where Γ depends both on the viscosity and the structural details of the CT through the Stokes-Einstein formula.

Minimizing the corresponding free energy functional, combining Eqs. 1–5 in the context of the Euler-Lagrange equation of motion, using scaled variables, and a traveling wave form for the CT pendula excitations, one obtains the following nonlinear ordinary differential equation governing the process

$$\frac{\mathrm{d}^2\eta}{\mathrm{d}\xi^2} + \beta\frac{\mathrm{d}\eta}{\mathrm{d}\xi} - \eta^3 + \eta + \varepsilon = 0 \tag{6}$$

where the following parameterization has been used

$$\begin{aligned}
\eta &= \frac{\theta}{\theta_0},\\
\xi &= \alpha(x - vt),\\
\beta &= \frac{\Gamma R v}{\sqrt{RJl\left(v_0^2 - v^2\right)}},\\
\varepsilon &= \frac{l\sqrt{\pi BR}\sin(2\gamma)\mu_{\text{p}}}{\sigma\left(Al/R - Rl\sigma\mu_{\text{p}}^2\cos^2\gamma\right)^{3/2}}E,\\
\sigma &= \left(\frac{\sin^2\gamma}{\chi_{\text{l}}} + \frac{\cos^2\gamma}{\chi_{\text{t}}}\right)^{-1},
\end{aligned} \tag{7}$$

where ξ is a moving coordinate, and $R = 12.5$ nm is the MT radius, $l = 4$ nm the length of a CT, γ the angle between $\vec{p}$ and $\vec{p}_{\text{t}}$ (see Fig. 1), $v_0 = 300$ m/s is the sound velocity in the medium, and v the velocity of kink excitations which amazingly emerges as special exact analytical solutions of this nonlinear ordinary differential equation with damping. This solution has been found earlier in a different context [60] and the reader is referred to it for a thorough mathematical analysis.

The most important consequence of Eq. 6 is the emergence of kink and anti-kink excitations resembling a domino-effect. The exact analytical form of the solution has the well-known hyperbolic tangent shape, (see Fig. 5)

$$\theta(\xi) = \pm\theta_0\tanh\left(\sqrt{2}\xi\right) \tag{8}$$

that propagates with a constant terminal velocity v_t obeying an analog of Ohm's law

$$v_t = \mu E \tag{9}$$

The kink's mobility μ depends on the model parameters, the ferroelectric features of MTs, and the elastic properties of CTs, as well as on viscous dissipation according to:

$$\mu = \frac{3v_0\sigma l^2\mu_{\text{p}}\sin(2\gamma)\sqrt{2\pi JB}}{2R\Gamma\left(Al/R - RL\sigma\mu_{\text{p}}^2\cos^2\gamma\right)} \tag{10}$$

Interestingly, this linear response law holds even for fields on the order of 10^5 V/m.

Thus, a kink involves several neighboring CTs which splay apart, much like wind-blown grass. This is due to the CTs having a dynamic electric dipole moment. We expect that a kink might influence motor proteins directly or through activation of co-ordinating proteins which thus regulate a corresponding class of motor proteins.

Even processive motors eventually unbind from the filament. This unbinding process can be characterized by an average walking time, which is on the order of seconds, and the corresponding walking distance, which is on the order of micrometers. Both quantities depend on the molecular roughness of MT filaments arising from the adsorbed tau protein or from the presence of unfavorable CT conformations. We argue that the presence of a kink

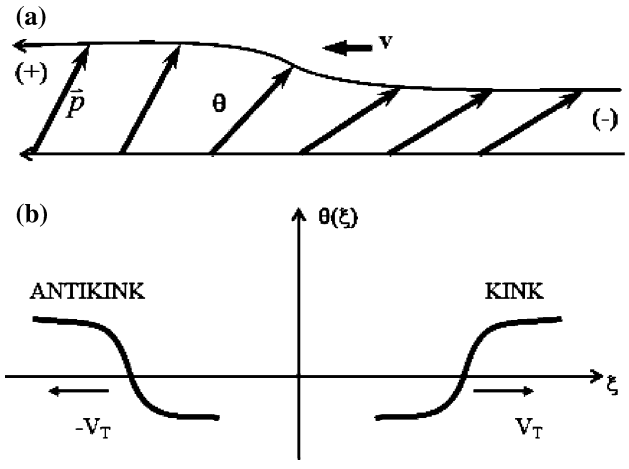

Fig. 5 **a** The kink's spatial dependence in terms of the local dipole moment's orientation. **b** The sketch of kink and anti-kink excitations

with the same direction of movement could help corresponding motor proteins to persist over longer walking distances.

How Intrinsic Electric Fields Could Control the Kink's Propagation

Let us first analyze the role of a constant intrinsic electric field (IDCF), E from (Fig. 1).

The most interesting case is presented by MTs in long neuron cells. Besides the chromosomes, many other large objects within the cell must be moved rapidly to particular locations by directed intra-cellular transport. The need for directed transport rather than reliance on simple diffusion and random walk processes is best understood in large cells, such as neurons. The longest neuron in the human body has a single thread-like projection (the axon) that reaches from the base of the spine to the foot, a distance of up to one meter.

Most cellular components, including large organelles, such as the aforementioned mitochondria, are synthesized within the cell body that lies in the spinal cord. They must be delivered down the axon to the synapse, where the neuron forms an electrically active connection with the muscles that flex the toe. One can estimate the time it would take for a mitochondrion to diffuse that distance to be on the order of 100 years! In fact, this journey is achieved in just a few days. Hence, there is a need for a mechanism other than simple unbiased diffusion.

The axon potential propagating along the neuron carries an electric field on the order of 10^4 V/m. This field, even when partially screened, oriented along MTs leads to the achievement of terminal velocities by kinks on the order of cm/s. We already stressed that experimental findings suggest opposite polarity motors are coordinated so that they usually do not interfere with each other's functions [61]. We propose that kinks are responsible for plus-end runs of kinesin while anti-kinks for switching to minus-end runs of dynein. Since they are much faster than loaded motors, such kinks (anti-kinks) can coordinate several motor proteins, producing enabling regions with strong transport in one direction.

Let us now estimate the speeds of kink (anti-kink) motions in MTs of nonneuronal cells. For a stable MT with a typical length $L = 4$ μm the IDCF in the central region of a MT can be calculated to be

$$E = \frac{Q}{\pi\varepsilon_0\varepsilon_r L^2} \tag{11}$$

Taking $Q = 13$ e, i.e. one excess charge per filament tip and letting the relative dielectric constant lie in the range $10 < \varepsilon_r < 80$ since it depends on the solution's composition, one finds the values of the resultant field to be in the range $(1 < E < 8)$ V/m resulting in the window of kink's terminal velocities to be given by

$$0.2\frac{\mu m}{s} < v_t < 1.6\frac{\mu m}{s} \tag{12}$$

Experimental evidence shows that depending on the ATP and salt concentration and the load placed on the kinesin molecule, it propagates along the MT with velocities ranging in the window $0 < v_t < 1$ μm/s, i.e. giving a healthy overlap with the velocities of biological motions that may interact with each other, (see Fig. 6). Let us focus now on the other important aspect of the possible role of electric fields in active transport along MTs.

It is believed that ordered (vicinal) water molecules generate an electric dipole field (WEDF) occurring on either side of the cell membrane. Within the interior of the cell the water molecules generate a WEDF in the vicinity of the cytoskeleton. Del Guidice et al. [62] have proposed that electromagnetic fields arising from WEDF coherent oscillations create electromagnetic signals comparable in size to the dimensions of MTs. These fields could couple with the already existing IDCFs in order to cooperatively control the kink's motion and consequently regulate the intense traffic of motor proteins along MTs.

This is particularly significant in view of the recent discovery of the existence of strong transient heterogeneous electric fields inside cells whose magnitudes can be comparable to those across membranes [63]. These fields can directly influence MTs located nearby which can subsequently transmit electrical signals throughout the cell using the mechanism proposed in the present paper. These electrical signaling mechanisms can be directly translated into the regulation of mass transport via motor proteins that propagate on microtubules.

Let us now consider the motion of a kink, Eq. 9, driven by a harmonic electric force generated by WEDF. We

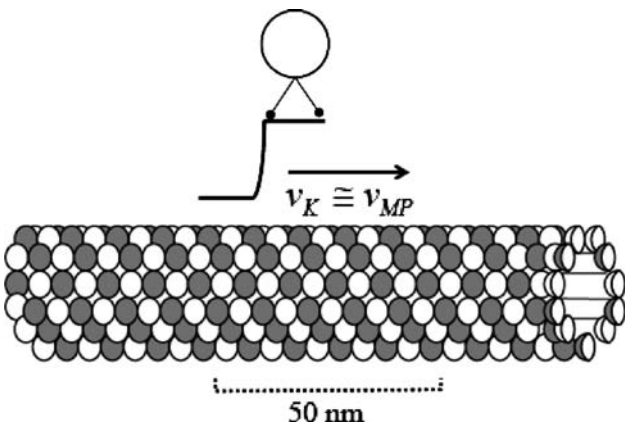

Fig. 6 The kink's velocity matches the kinesin's propagation speed and hence kinesin is "surfing" on it

assume that the dimensionless driving force has a wavelength that is greater than the average MT length and it harmonically depends on time τ as:

$$f(\tau) = f_0 \cos(\Omega\tau + \varphi_0) \tag{13}$$

Henceforth, we will term it the intrinsic alternative current field WEDF, where f_0 is the amplitude, Ω the frequency, and φ_0 the initial phase of the driving force. Adding Eq. 13 to Eq. 6 we could examine numerically the kink's dynamics in the new regime. First we examined the case where a strong IDCF, carried by the action potential in a nerve cell, is switched on in parallel with the harmonic WEDF, Eq. 14. An examination based on our model Eqs. 6, 7 provides the order of magnitude for the damping and forcing parameters, respectively as $\beta = 0.001$ and $\varepsilon = 0.01$. Choosing $f_0 = 0.01$ and $\Omega = 0.01$, with the initial conditions $\varphi_0 = 0$ and $\frac{d\eta}{d\tau}(0) = 0$, we find that the kink's uni-directional motion on entering the terminal regime attains the dimensionless speed of $v = 0.00004$, (see Fig. 7a). The actual kink speed is on the order of $v_k = v \cdot v_0 \approx 1$ cm/s.

If the initial phase of WEDF is $\varphi_0 = \frac{\pi}{2}$, under the same remaining conditions, uni-directional kink motion is faster ($v = 0.0001$, $v_k \approx 3$ cm/s) and accompanied by oscillations (Fig. 7b). When the initial phase is $\varphi_0 = -\frac{\pi}{2}$ the direction of motion reverses and proceeds with velocity $v = 0.00006$, (Fig. 7c). By increasing the amplitude of WEDF to $f_0 = 0.1$ the velocity of uni-directional motion does increase too (Fig. 7d). The uni-directional oscillating motion is a combined effect of influences from AC and DC fields, so it may depend on the frequency and even on the initial phase, which is the most striking effect of our simulations. In Figs. 7 and 8, we use dimensionless axes such that the slope of the graph gives a dimensionless velocity, as introduced above. The actual velocity can be found through the scaling relationship $v_k = v \cdot v_0$ where v_0 is the speed of sound.

If the intrinsic field E is weaker, say on the order of a few (V/m), we test the kink's dynamics for a comparable set of parameters, namely: ($\beta = 0.001$, $\varepsilon = 0.0002$, $f_0 = 0.01$, $\Omega = 0.01$, $\varphi_0 = -\frac{\pi}{2}$, $\frac{d\eta}{d\tau}(0) = 0$). The uni-directional motion of the kink is now slower and accompanied by oscillations of the same frequency (Fig. 8a). Under realistic conditions it is expected that the kink has a nonzero initial velocity. Put under the same other conditions $\left(\frac{d\eta}{d\tau}(0) = 0.001\right)$ the average kink's velocity is the same but the oscillations are more conspicuous (Fig. 8b). Eventually if the frequency of WEDF is increased, the velocity of the uni-directional motion of the kink is lowered ($v = 0.00005$) and the amplitude of oscillations is increased, (Fig. 8c).

The numerical evidence presented here suggests that the combined action of IDCF and WEDF can control the direction, the velocity, and the frequency of the superimposed oscillations of the kinks involved. This makes these fields a powerful means for tuning the kink's dynamics and consequently creating their catalytic roles in the regulation of motor protein traffic.

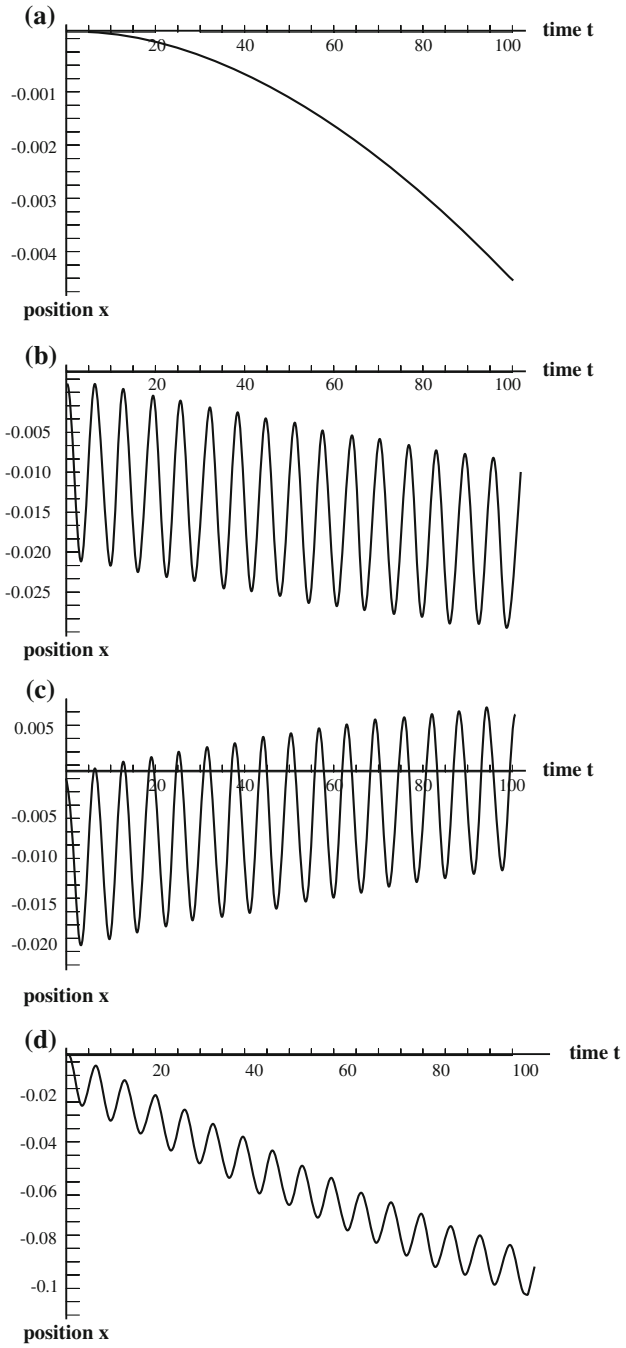

Fig. 7 The kink movement governed by the force of IDCF ($\varepsilon = 0.01$) and coupled with WEDF with the dimensionless frequency $\omega = 0.01$, $\eta' = 0$, and $\beta = 0.001$, with amplitude f_0 and initial phase φ_0 as follows: **a** $f_0 = 0.01$, $\varphi_0 = 0$ **b** $f_0 = 0.01$, $\varphi_0 = \frac{\pi}{2}$ **c** $f_0 = 0.01$, $\varphi_0 = -\frac{\pi}{2}$ **d** $f_0 = 0.1$, $\varphi_0 = \frac{\pi}{2}$

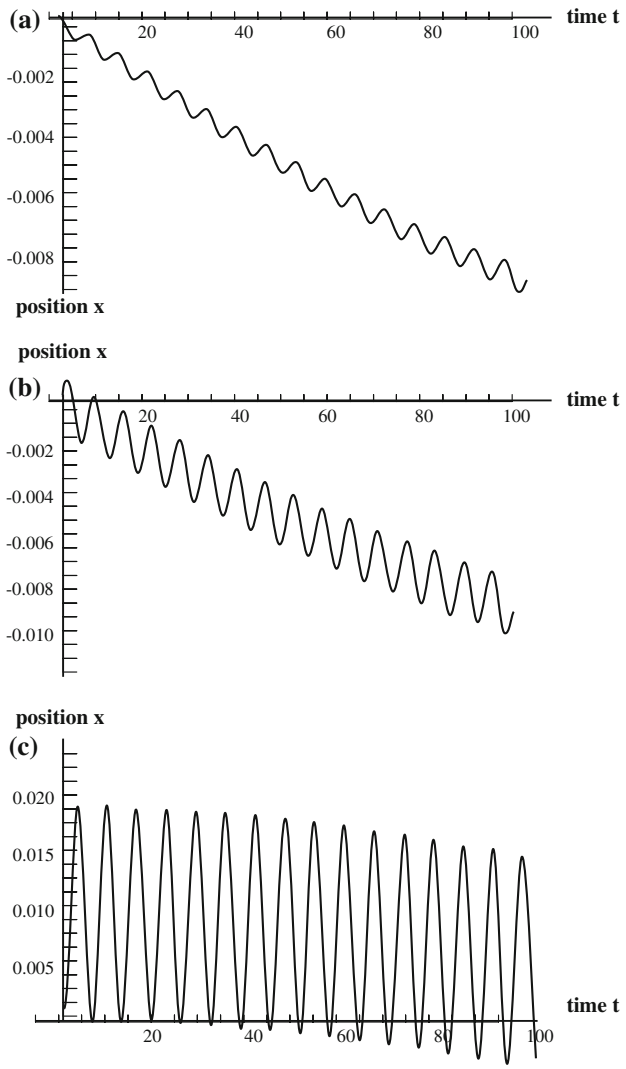

Fig. 8 The kink movement governed by the force of IDCF ($\varepsilon = 0.0002$) and coupled with WEDF with the amplitude $f_0 = 0.01$, initial phase $\varphi_0 = \frac{\pi}{2}$, and dimensionless frequency **a** $\omega = 0.01, \eta' = 0$ **b** $\omega = 0.01, \eta' = 0.001$ **c** $\omega = 0.05, \eta' = 0$

There is ample experimental evidence indicating that endocytic vesicles exhibit an oscillatory bi-directional process along MTs [64]. It could be attributed to the control mechanism provided by oscillating kinks as described above.

It is worth noting that the general analysis of this mechanism was first introduced by Savin et al. [65].

Discussion and Conclusions

In this paper we have argued that the GTP hydrolysis taking place as a result of tubulin assembly into MTs is involved in a chemical energy transduction as a combination of mechanical and electrical energy propagating along the MT axis in the form of a kink excitation. The first point made in this connection was the difference in the electrical properties of the two MT ends [17] that leads to the emergence of ferroelectric properties of MTs. Moreover, it creates IDCF along the MT axis. The intensity of IDCF depends on the length of the MT as well as on the physiological conditions of the solution and on the presence or absence of action potentials (neurons).

We then turned our attention to the role played by MTs in motor protein transport involving the kinesin and dynein superfamilies. How are proteins, with their very diverse functional roles in the cell, able to produce mesoscopic and even macroscopic movements in a co-ordinated fashion? The answer to this question is still largely unknown. For example, the formation of the mitotic spindle apparatus and the process of chromosome segregation require concerted efforts of force generation by kinetochore MTs and a simultaneous action of kinesin and dynein motors. In a process as important as cell division, mistakes that would be a frequent occurrence if random thermal fluctuations were to rule, must be necessarily eliminated.

Within the framework of our model proposed in this paper, MTs are not only passive tracks for mass transport in the cell but also signal relays for electrical, mechanical, and chemical stimuli that may be transduced over distances comparable to the cell size. Additionally, the cell can control the amplitude, frequency, and the phase of the electric field induced in a MT by changing *WEDF*, ionic concentrations or pH values. It is expected that the combined action of *IDCF* and *WEDF* resulting in unidirectional translation accompanied by oscillations could enable stuck cargoes to back up, thus getting them out of potential traffic jams [66]. For instance, moving down an axon, a cargo might encounter a blocked MT (e.g. with too many microtubule-associated proteins bound to it, preventing the motor from continuing on its way). If the opposite motors where switched on, the cargo would reverse its course and then switch to a second MT that crossed the path of the first.

It is quite feasible that local dipolar fields carried by a kink could play the role of a switch which turns off one class of motors and turns on another. Then, the cargo enabled with both kinds of motors could be ready to go in either direction at any time. The decision as to which direction should be chosen would depend on the kink encountering the particular cargo.

It should be kept in mind that even processive motor proteins (MP) eventually unbind from the MT. This unbinding process can be characterized by an average walking time, which is on the order of seconds, and the corresponding walking distance which is on the order of micrometers. It was found experimentally [67] that the on-rates and off-rates of the engaged MPs can be regulated via their interactions with various proteins or due to other

factors which affect cargo processivity by providing additional links between the cargo and the MT. For instance, kinesin-MT binding is strongly ionic and hence very sensitive to MT charge distribution which dramatically depends on pH, for example [68]. We argue that the presence of a kink with an appropriate direction and speed of movement could help in the regulation of MP-MT affinity and result in the MP persisting over longer distances in its walk. On the other hand, it could cause oppositely moving MPs to disengage from the same MT protofilament thus avoiding the emergence of potential traffic jams. The applied load could significantly reduce the distance over which a single MP would be expected to transport the cargo, as well as how fast it would go. In that case the action of appropriate kinks should re-engage detached MPs and hence sustain active transport. It is likely that kinks may arrange multiple MPs of the same class resulting in a longer mean processive distance for the "ordered" MPs carrying cargos to a location where they are needed.

In summary, the hypothesis and model presented in this paper offer new insights into intracellular molecular processes related to MT dynamics. Some of the predictions made here can be tested with experimental tools such as M̈ossbauer spectroscopy [11] and neutron scattering with deuterium labeling that would enable the verification of the magnitude of CT conformational changes and their kink propagation along MT [69]. However, these experimental techniques are much more subtle than those used for protein structure determination, which are preformed at low temperatures.

Acknowledgments This work was supported by the Serbian Ministry of Science and Technology under project F141018A awarded to the Serbian authors, and by a Natural Sciences and Engineering Research Council of Canada (NSERC) grant awarded to J.A.T.

References

1. Lang, S. B. (1998). In A. A. Marino (Ed.), *Modern Bioelectricity* (p. 243). New York: Marcel Dekker, Inc.
2. Leuchtag, H. R. & Bystrov, V. S. (1999). Theoretical models of conformational transitions and ion conduction in voltage-dependent ion channels: Bioferroelectricity and superionic conduction. *Ferroelectrics, 220*, 157 and references therein.
3. Fong, P. (1968). RNA as a ferroelectric recording tape for brain memory. *Bulletin of the American Physical Society, 13*, 613.
4. Ionov, S. P., & Ionova, G. V. (1972). Model of a biological membrane with tunnel chemical bonds. *Doklady Biophysics, 202*, 22.
5. Kubisz, L., Jozwiak, G., Jaroszyk, F., Tuliszka, M., & Kudynski, R. (1984). Studies of ferroelectric properties of collagen. *Acta Physiologica Polonica, 35*(5–6), 571–576.
6. Fukada, E., Ueda, H., & Rinaldi, R. (1976). Piezoelectric and related properties of hydrated collagen. *Biophysical Journal, 16*, 911–918.
7. Athenstead, H. (1974). Pyroelectric and piezoelectric properties of vertebrates. *Annals of the New York Academy of Sciences, 238*, 68–94.
8. Leuchtag, H. R., & Bystrov, V. S., editors. (1999). Special issue on Ferroelectrics and related models in biological systems. *Ferroelectrics, 220*(3–4), V–VI.
9. Hol, W. G. (1985). The role of the alpha-helix dipole in protein function and structure. *Progress in Biophysics and Molecular Biology, 45*, 149–195.
10. Satarić, M. V., Tuszyński, J. A., & Žakula, R. B. (1993). Kinklike excitations as an energy-transfer mechanism in microtubules. *Physical Review E, 48*, 589–597.
11. Satarić, M. V., Zeković, S., Tuszyński, J. A., & Pokorny, J. (1998). Mössbauer effect as a possible tool in detecting nonlinear excitations in microtubules. *Physical Review E, 58*(5), 6333–6339.
12. Satarić, M. V., & Tuszyński, J. A. (2003). Models of spatial and orientational self-organization of microtubules under the influence of gravitational fields. *Physical Review E, 67*(1–11), 011901.
13. Alberts, et al. (1994). *Molecular biology of the Cell*. New York: Garland Publishing.
14. Brown, J. A., & Tuszyński, J. A. (1999). A review of the ferroelectric model of microtubules. *Ferroelectrics, 220*, 141.
15. Trpisova, B., & Tuszyński, J. A. (1997). Possible link between guanosine 5^{IIH} triphosphate hydrolysis and solitary waves in microtubules. *Physical Review E, 55*, 3288–3302.
16. Tuszyński, J. A., Luchko, T., Carpenter, E., & Crawford, E. (2004). Results of molecular dynamics computations of the structural and electrostatic properties of tubulin and their consequences for microtubules. *Journal of Theoretical and Computational Nanoscience, 1*, 392–397.
17. Baker, N. A., Sept, D., Joseph, S., Holst, M. J., & McCammon, J. A. (2001). Electrostatics of nanosystems: Application to microtubules and the ribosome. *Proceedings of the National Academy of Sciences of the United States of America, 98*, 10037–10041.
18. Maniotis, A. J., Chen, C. S., & Ingber, D. E. (1997). Demonstration of mechanical connections between integrins, cytoskeletal filaments, and nucleoplasm that stabilize nuclear structure. *Proceedings of the National Academy of Sciences of the United States of America, 94*, 849–854.
19. Tuszyński, J. A., Carpenter, E. J., Crawford, E., Brown, J. A., Malinski, W., & Dixon, J. M. (2003). In W. Badawy, & W. Moussa (Eds.), *Proceedings of ICMENS 2003, International Conference on MEMS, NANO and Smart Systems, Banff* (pp. 55–61). Los Alamitos, California: IEEE Computer Society.
20. Mershin, A., Kolomenskii, A. A., Nanopoulos, D. V., & Schuessler, H. A. (2004). Tubulin dipole moment, dielectric constant and quantum behavior: Computer simulations, experimental results and suggestions. *Biosystems, 77*(1–3), 73–75.
21. Schuessler, H. A., Mershin, A., Kolomenskii, A. A., & Nanopoulos, D. V. (2003). Surface plasmon resonance study of the actin-myosin sarcomeric complex and tubulin dimers. *Journal of Modern Optics, 50*, 2381–2391.
22. Pokorny, J., Jelinek, F., & Trkal, V. (1998). Electric field around microtubules. *Bioelectrochemistry and Bioenergetics, 45*, 239–245.
23. Jelinek, F., Pokorny, J., Saroch, J., Trkal, V., Hasek, J., & Palan, B. (1999). Microelectronic sensors for measurement of electromagnetic fields of living cells and experimental results. *Bioelectrochemistry and Bioenergetics, 48*, 261–266.
24. Stracke, R., Boehm, K. J., Wollweber, L., Unger, E., & Tuszyński, J. A. (2002). Analysis of the migration behaviour of single microtubules in electric fields. *Biochemistry and Biophysics Research Communications, 293*, 602–609.
25. Sanabria, H., Miller, J. H., Mershin, A., Luduena, R. F., Kolomenski, A. A., Schuessler, H. A., et al. (2006). Impedance spectroscopy of a-b tubulin heterodimer suspensions. *Biophysics Journal, 90*, 4644–4650.

26. Dombeck, D. A., Kasischke, K. A., Vishwasrao, H. D., Ingelsson, M., Hyman, B. T., & Webb, W. W. (2003). Uniform polarity microtubule assemblies imaged in native brain tissue by second-harmonic generation microscopy. *Proceedings of the National Academy of Sciences of the United States of America, 100*(12), 7081–7086.
27. Gagliardi, L. (2002). Electrostatic force in prometaphase, metaphase, and anaphase-A chromosome motions. *Physical Review E, 66*, 011901.
28. Nanopoulos, D. V., Mavromatos, N. E., & Zioutas, K. (1998). Ferroelectrics and their possible involvement in biology. *Advances in Structural Biology, 5*, 127–137.
29. Weitzel, E. K., Tasker, R., & Brownell, W. E. (2003). Outer hair cell piezoelectricity: Frequency response enhancement and resonance behavior. *The Journal of the Acoustical Society of America, 114*, 1462–1466.
30. Tuszyński, J. A., Brown, J. A., Crawford, E., Carpenter, E. J., Nip, M. L. A., Dixon, J. M., et al. (2005). Molecular dynamics simulations of tubulin structure and calculations of electrostatic properties of microtubules. *Mathematical and Computer Modelling, 41*(10), 1055–1070.
31. Hodgkin, A. L., & Huxley, A. F. (1952). Currents carried by sodium and potassium ions through the membrane of the giant axon of Loligo. Journal of Physiology (London 116, 449, 473 and 497) (1952; 117, 500).
32. Howard, J. (1996). The movement of kinesin along microtubules. *Annual Review of Physiology, 58*, 703–729.
33. Hackney, D. D. (1996). The kinetic cycles of myosin, kinesin, and dynein. *Annual Review of Physiology, 58*, 732–750.
34. Hackney, D. D. (1995). Motor proteins, polar explorations. *Nature, 376*, 215–216.
35. Cole, D. G., & Scholey, J. M. (1995). Structural variations among the kinesins. *Trends in Cell Biology, 5*, 259–262.
36. Leibler, S., & Huse, D. A. (1993). Porters versus rowers: A unified stochastic model of motor proteins. *The Journal of Cell Biology, 121*, 1357–1368.
37. Brown, J. A., & Tuszyński, J. A. (1997). Dipole interactions in axonal microtubules as a mechanism of signal propagation. *Physical Review E, 56*, 5834–5840.
38. Woehlke, G., Ruby, A. K., Hart, C. L., Ly, B., Hom-Booher, N., & Vale, R. D. (1997). Microtubule interaction site of the kinesin motor. *Cell, 90*, 207–216.
39. Julicher, F., Adjari, A., & Prost, J. (1997). Modeling molecular motors. *Review of Modern Physics, 69*, 1269–1281.
40. Ruppel, K. M., Lorenz, M., & Spudich, J. A. (1995). Myosin structure/function: A combined mutagenesis-crystallography approach. *Current Opinions in Structural Biology, 5*, 181–186.
41. Buttiker, M. (1987). Transport as a consequence of state-dependent diffusion. *Zeitschrift für Physik B, 68*, 161.
42. Landauer, R. (1988). Motion out of noisy states. *Journal of Statistical Physics, 53*, 233.
43. Feynman, R. P., Leighton, R. B., & Sands, M. (1963). *The Feynman lectures on physics* (Vol. 1). Reading, Massachusetts: Addison-Wesley Publ. Co.
44. Doering, C. R., Horsthemke, W., & Riordan, J. (1994). Nonequilibrium fluctuation-induced transport. *Physical Review Letters, 72*, 2984.
45. Astumian, R. D., & Bier, M. (1994). Fluctuation driven ratchets: Molecular motors. *Physical Review Letters, 72*, 1766.
46. Risken, H. (1989). *The Fokker-Planck equation*. Berlin: Springer-Verlag.
47. Svoboda, K., & Block, S. M. (1994). Force and velocity measured for single kinesin molecules. *Cell, 77*, 773.
48. Bolterauer, H., Tuszyński, J. A., & Unger, E. (2005). Directed binding: A novel physical mechanism that describes the directional motion of two-headed kinesin motor proteins. *Cell Biochemistry and Biophysics, 42*, 95–119.
49. Gross, S. P., Vershinin, M., & Shubeita, G. T. (2007). Cargo transport: Two motors are sometimes better than one. *Current Biology, 17*, R478–R486.
50. Mallik, R., & Gross, S. P. (2006). Molecular motors as cargo transporters in the cell—The good, the bad and the ugly. *Physica A, 372*, 65–69.
51. Nogales, E., Wolf, S. G., & Downing, K. H. (1998). Structure of the alpha beta tubulin dimer by electron crystallography. *Nature, 391*, 199–203.
52. Jiminez, M. A., Evangelio, J. A., Aranda, C., Lopez-Braet, A., Andreu, D., Rico, M., et al. (1999). Helicity of alpha(404–451) and beta(394–445) tubulin C-terminal recombinant peptides. *Protein Science, 8*, 788–799.
53. Sackett, D. L. (1995). Structure and function in the tubulin dimer and the role of the acid carboxyl terminus. In B. B. Biswas & S. Roy (Eds.), *Subcellular biochemistry-proteins: Structure, function and engineering* (Vol. 24, pp. 255–302). Dordrecht: Kluwer Academic Publishers.
54. Wang, Z., & Sheetz, M. P. (2000). The C-terminus of tubulin increases cytoplasmic dynein and kinesin processivity. *Biophysics Journal, 78*, 1955–1964.
55. Manning, G. (1978). The molecular theory of polyelectrolyte solutions with applications to the electrostatic properties of polynucleotides. *Quarterly Reviews of Biophysics, 2*, 179–246.
56. Tuszyński, J. A., Priel, A., & Woolf, N. (2005). Transitions in microtubule c-termini conformations as a possible dendritic signaling phenomenon. *European Biophysics Journal, 35*(1), 40–52.
57. Vale, R. D., & Milligan, R. A. (2000). The way things move: Looking under the hood of molecular motor proteins. *Science, 288*, 88–95.
58. Satarić, M. V., Satarić, B. M., & Tuszyński, J. A. (2005). Nonlinear model of microtubule dynamics. *Electromagnetic Biology and Medicine, 24*, 255–264.
59. Satarić, M. V., Matsson, L., & Tuszyński, J. A. (2006). Complex movements of motor protein relay helices during the power stroke. *Physics Review E, 74*, 051902.
60. Dixon, J. M., Tuszynski, J. A., & Otwinowski, M. (1991). Special analytical solutions of the damped anharmonic oscillator equation. *Physics Review A, 44*, 3484–3491.
61. Heintzelman, M. B. (2003). Gliding motility: The molecules behind the motion. *Current Biology, 13*, R57–R59.
62. Del Guidice, E., Preparata, G., & Vitiello, G. (1988). Water as a free electron dipole laser. *Physical Review Letters, 61*, 1085–1088.
63. Tyner, K. M., Kopelman, R., & Philbert, M. A. (2007). "Nano-sized Voltmeter" enables cellular-wide electric field mapping. *Biophysics Journal, 93*, 1163–1174.
64. Murray, J. W., Bananis, E., & Wolkoff, A. W. (2000). Reconstitution of ATP-dependent movement of endocytic vesicles along microtubules in vitro: An oscillatory bidirectional process. *Molecular Biology of the Cell, 11*, 419–433.
65. Savin, A. V., Tsironis, G. P., & Zolotaryuk, A. V. (1997). Ratchet and switching effects in stochastic kink dynamics. *Physics Letters A, 229*, 279.
66. Gross, S. P. (2004). Hither and yon: A review of bi-directional microtubule-based transport. *Physical Biology, 1*, R1–R11.
67. Reed, N. A., Cai, D., Blasius, T. L., Jih, G. T., Meyhofer, E., Gaerting, J., et al. (2006). Microtubule acetylation promotes kinesin–1 binding and transport. *Current Biology, 16*, 2166–2172.
68. Zaccai, G. (2000). How soft is a protein? A protein dynamics force constant measured by neutron scattering. *Science, 208*, 1604–1607.
69. Humphrey, W., Dalke, A., & Schulten, K. (1996). VMD—visual molecular dynamics. *Journal of Molecular Graphics, 14*, 33–38.